Title

Topological reorganization of functional hubs in patients with Parkinsons disease with freezing of gait.

Journal

Journal of Neuroimaging, 33(4)

Authors

Sreenivasan, Karthik
Zhuang, Xiaowei
Longhurst, Jason
et al.

Publication Date

2023

DOI

10.1111/jon.13107

Peer reviewed

HHS Public Access

Author manuscript

J Neuroimaging. Author manuscript; available in PMC 2023 September 27.

Published in final edited form as:

J Neuroimaging. 2023 ; 33(4): 547–557. doi:10.1111/jon.13107.

Topological reorganization of functional hubs in patients with Parkinson's disease with freezing of gait

Karthik Sreenivasan[1], **Ece Bayram**[2], **Xiaowei Zhuang**[1], **Jason Longhurst**[3], **Zhengshi Yang**[1], **Dietmar Cordes**[1,4], **Aaron Ritter**[1], **Jessica Caldwell**[1], **Jeffrey L. Cummings**[5], **Zoltan Mari**[1], **Irene Litvan**[2], **Brent Bluett**[6], **Virendra R. Mishra**[1,7]

[1]Cleveland Clinic Lou Ruvo Center for Brain Health, Las Vegas, Nevada, USA

[2]Department of Neurosciences, University of California San Diego, La Jolla, California, USA

[3]Department of Physical Therapy and Athletic Training, Saint Louis University, St. Louis, Missouri, USA

[4]Department of Radiology, University of Colorado Boulder, Boulder, Colorado, USA

[5]Chambers-Grundy Center for Transformative Neuroscience, Department of Brain Health, School of Integrated Health Sciences, University of Nevada, Las Vegas, Nevada, USA

[6]Central California Movement Disorders, Pismo Beach, California, USA

[7]Department of Radiology, Heersink School of Medicine, The University of Alabama at Birmingham, Birmingham, Alabama, USA

Abstract

Background and Purpose: Resting-state functional MRI (rs-fMRI) studies in Parkinson's disease (PD) patients with freezing of gait (FOG) have implicated dysfunctional connectivity over multiple resting-state networks (RSNs). While these findings provided network-specific insights and information related to the aberrant or altered regional functional connectivity (FC), whether these alterations have any effect on topological reorganization in PD-FOG patients is incompletely understood. Understanding the higher order functional organization, which could be derived from the "hub" and the "rich-club" organization of the functional networks, could be crucial to identifying the distinct and unique pattern of the network connectivity associated with PD-FOG.

Methods: In this study, we use rs-fMRI data and graph theoretical approaches to explore the reorganization of RSN topology in PD-FOG when compared to those without FOG. We also compared the higher order functional organization derived using the hub and rich-club measures

Correspondence: Virendra R. Mishra, Department of Radiology, Heersink School of Medicine, The University of Alabama at Birmingham, Volker Hall G078D, 1670 University Blvd, Birmingham, AL 35233, USA. virendrarmishra@uabmc.edu.

CONFLICT OF INTEREST STATEMENT

The authors declare no conflicts of interest.

in the FC networks of these PD-FOG patients to understand whether there is a topological reorganization of these hubs in PD-FOG.

Results: We found that the PD-FOG patients showed a noticeable reorganization of hub regions. Regions that are part of the prefrontal cortex, primary somatosensory, motor, and visuomotor coordination areas were some of the regions exhibiting altered hub measures in PD-FOG patients. We also found a significantly altered feeder and local connectivity in PD-FOG.

Conclusions: Overall, our findings demonstrate a widespread topological reorganization and disrupted higher order functional network topology in PD-FOG that may further assist in improving our understanding of functional network disturbances associated with PD-FOG.

Keywords

freezing of gait; functional connectivity; functional magnetic resonance imaging; graph theory; Parkinson's disease

INTRODUCTION

Freezing of gait (FOG) is defined as a brief, episodic absence or marked reduction of the forward progression of feet despite the intention to walk.[1] Parkinson's disease (PD) patients with freezing of gait (FOG) experience a feeling that their feet are "glued" to the floor and are unable to move.[1] PD-FOG is considered one of the most debilitating motor symptoms affecting almost 50% of patients with PD[2,3] and is one of the most common causes of falls and subsequent morbidity and mortality.[4] Several competing hypotheses have been proposed such as the threshold model that assumes that when certain parameters of gait are at a motor breakdown threshold, then FOG dominates[5]; the interference model that assumes that FOG dominates when there is an interference between the motor, cognitive, and limbic brain networks[6]; the cognitive model that emphasizes the conflict-resolution deficit that may be responsible for FOG[7]; and the decoupling model that assumes the occurrence of FOG due to disconnection between the pre-planned motor program and motor response.[8] However, these models are incomplete and only partially explain the phenotype of PD-FOG. In general, FOG has been attributed to overloading across neural networks in an attempt to compensate for reduced motor function,[9–12] which may lead to the inability to "set-shift" among the different neural networks.[12]

Neuroimaging studies utilizing resting-state functional MRI (rs-fMRI) in PD-FOG have implicated altered connectivity in the motor and nonmotor pathways and dysfunctional connectivity between cortical and subcortical regions over multiple resting-state networks (RSNs).[13,14] Specifically, resting-state functional connectivity (rs-FC) involving the frontoparietal network (FPN) and visual network has been thought to be altered in PD-FOG and this disruption of connectivity between RSNs was correlated with the Freezing of Gait Questionnaire (FOGQ).[13] Recent studies have augmented these findings and have shown the involvement of the sensorimotor, dorsal attention, and default mode networks.[15,16]

Rs-fMRI has also been utilized to study large-scale topological organization through graph-theoretical modeling.[17] Advances in the application of graph-theoretical methods have enabled us to characterize unbiased whole-brain connectivity at global and local levels and

gain insights into the topological organization of the human brain networks.[17–20] Previous studies have demonstrated large-scale network changes from early brain development[21] to healthy aging[22] and various neurodegenerative diseases.[23–29] Graph-theoretical approaches can be used to study various network measures that can inform about both network segregation and integration.[30] However, limited existing studies have adopted a whole-brain unbiased approach to study network-level connectivity differences related to PD-FOG. Exploratory whole-brain unbiased graph-theoretical studies in PD-FOG have shown altered topological organization at the network and regional levels.[15,31,32] For instance, PD-FOG participants have also shown reduced efficiency of the dorsal attention network[16] as compared to PD participants without FOG (PD-nFOG) and normal controls (NCs). However, such network-specific insights do not explain the higher order functional organization, which could be derived from the "hub" and the "rich-club" organization of the functional networks.

Nodes in a network that are identified as hubs or part of a rich-club are proposed to be vital for global network integration and coordination.[33,34] The hub nodes play an important role in global integration and the rich-club organization and can provide insights into the network's resilience, hierarchical ordering, and specialization.[33,34] Subsequently, given that PD-FOG is associated with the inability to "set-shift" among different networks,[12] understanding the role of key hub-like regions that play an important role in the efficient global integration of brain functional networks could be crucial to identifying the distinct and unique pattern of the network connectivity associated with PD-FOG.

In this study, we used high-temporal-resolution rs-fMRI data to investigate whether there are discernible topological organization differences between PD-FOG and PD-nFOG. We applied the graph-theoretical approach to the functional connectivity (FC) data derived using rs-fMRI and first compared global and local graph-theoretically derived topological measures of efficiency between the groups, and evaluated whether these measures were different between the two groups. We also computed and compared hub and rich-club measures in the FC networks of these PD-FOG participants to understand whether there is a topological reorganization of these hubs in PD-FOG participants. Finally, we tested for correlation between the clinical measures and graph-theoretical derived methods to explore whether changes in the graph-theoretical measures can predict the clinical outcomes of FOG.

METHODS

Data used for this study were obtained from the Center for Neurode-generation and Translational Neuroscience (CNTN) database (www.nevadacntn.org). The current study was approved by the institutional review board of Cleveland Clinic and all subjects provided informed written consent. The inclusion criteria for patients with PD in this study was a diagnosis of PD based on the United Kingdom Parkinson's Disease Society Brain Bank Diagnostic Criteria.[35] PD participants were evaluated for FOG with a self-report measure (FOGQ) and a comprehensive battery of clinical tests (FOG score[36] including Timed Up and Go and Movement Disorders Society-Unified Parkinson's Disease Rating Scale [MDS-UPDRS III]). These assessments were recorded and reviewed by three members of the

research team (two movement disorders specialists and one physical therapist with expertise in FOG) to confirm the presence or absence of FOG. Participants were classified to have FOG if they were observed to have an FOG episode during any of the clinical assessments for FOG.

Thirty-eight PD participants were recruited; 17 participants were identified as PD-FOG and 21 as PD-nFOG. Of these, one PD-FOG and five PD-nFOG participants were identified as outliers based on MDS-UPDRS III scores more than 3 scaled median absolute deviation away from the median of the respective group and were removed from further analysis. We included 16 age-, sex-, and education-matched NCs from the CNTN cohort as a comparison group. We obtained general demographics for all subjects and the disease duration, Montreal Cognitive Assessment (MoCA), Geriatric Depression Scale (GDS), State-Trait Anxiety Inventory (STAI), FOGQ score, Hoehn and Yahr scale, levodopa equivalent doses (LEDD), and MDS-UPDRS-III scores (tremor and postural instability/gait difficulty [PIGD] subscores) for each patient with PD (Table 1).

All subjects underwent rs-fMRI scans on a 3T Siemens Skyra scanner. A 32-channel head coil was used for data acquisition, and all PD participants were scanned in the clinically defined “ON” state. The rs-fMRI involved gradient-echo T2*-weighted echo-planar imaging (EPI) acquisition with 850 dynamics (repetition time [TR] = 700 ms, echo time [TE] = 28.4 ms, flip angle = 42°, resolution = 2.3 × 2.3 × 2.3 mm^3, 64 axial slices, multiband = 8, and phase encoding = posterior [P] >> Anterior [A]). We acquired spin-echo EPI images with the same parameters in the same and opposite phase encoding (P >> A and A >> P, respectively) for distortion correction. A high-resolution (1 × 1 × 1 mm^3) T1-weighted structural image was acquired for each subject using a 3-dimensional T1-weighted gradient echo with magnetization-prepared 180° radio-frequency pulses and rapid gradient-echo sequence (TR = 2300 ms, TE = 2.96 ms, flip angle = 9°).The total time of acquisition was approximately 18 minutes.

The first 15 time frames (10 seconds) were removed to allow the MR signal to achieve T1 equilibrium. Time frames were distortion corrected, slice-time corrected, and realigned to the mean image using the statistical parametric mapping (http://www.fil.ion.ucl.ac.uk/spm/), further co-registered to the subject T1-space, and then normalized to the standard Montreal Neurological Institute-152 2-mm template using advanced normalization tools (http://stnava.github.io/ANTs/). A total of 246 different cortical regions of interest (ROIs) were identified based on the Brainnetome functional atlas.[37] The first principal component resulting from the singular value decomposition of all the time series within the ROI mask was defined as the time series for the ROI. Six motion parameters and their derivatives, as well as CompCor-generated white matter and cerebrospinal signals,[38] were regressed from the extracted time series. All voxel time series were bandpass filtered ($0.008 < f < 0.1$ Hz) to emphasize low-frequency correlations in the resting state, and then variance was normalized. Root-mean-square (RMS) head motion was computed for every subject.

The extracted and preprocessed time series were then used to obtain FC matrices for all participants. The Pearson correlation coefficient between the time series for each pair of ROIs was calculated and the correlation matrix was obtained for each subject.

Graph-theoretical measures were used to study the topological properties of functional networks in the different groups. The correlation matrices obtained were thresholded by sorting all the edges by weight (highest correlation to lowest correlation) and only retaining the top S% of edges (S = sparsity). Subsequently, we ensured that the thresholded set of weighted graphs (graphs with edges weighted by Pearson's correlation coefficient) being compared had the same number of edges to determine unbiased between-group differences in network organization.[39] Only positive correlation values (r-values) were used for the analysis. The thresholding was applied for a range of S values with an interval of .01. The lower limit of .1 (10%) was chosen such that nodes that are isolated from the rest of the network are minimal, and the upper limit of .5 (50%) was chosen to suppress the contribution of spurious correlations, similar to the previous studies.[29,40] Graph-theoretical measures used to compare group differences were obtained using custom Matlab® scripts and a graph-theoretical network analysis toolbox.[41]

The network measures of interest, namely (1) small-world properties (including normalized clustering coefficient [γ] and normalized characteristic path length [λ]), (2) network efficiency involving local efficiency (Eloacl) and global efficiency (Eglobal), (3) network strength (D), and (4) assortativity (A)[17] were calculated for the weighted graphs at each S. In addition, we also estimated the hub disruption index[42] and the rich-club properties.[33]

Small-world properties

Small-world properties were originally proposed by Watts and Strogatz.[43] It involves the determination of the clustering coefficient (C), characteristic path length (L), γ, and λ. C denotes the extent of local interconnectivity or cliquishness in the network and was measured by taking the average of clustering coefficients across all nodes in the network. γ was computed by normalizing each graph's C by C_{random} (mean C of 100 matched random networks). L of the network was computed as the average of the shortest path length, averaged over all pairs of nodes in the network. λ was computed by normalizing each graph's L by L_{random} (mean L_{nw} of 100 matched random networks). The small-worldness of a network can be expressed as $\sigma = \gamma/\lambda$, which is typically larger than 1 in the case of a small-world organization ($\sigma > 1$, $\gamma > 1$, and $\lambda \sim 1$).[20,43] It represents both efficient network segregation and network integration.[30]

Network efficiency

Network efficiency was studied by obtaining local (E_{local}) and global efficiency (E_{global}) of the connectivity networks. The global efficiency E_{global} of the network measures the efficiency of the parallel information transfer and is given by the average of the inverse shortest path between the nodes in the network. E_{local} represents how well local subgraphs (subnetwork) exchange information when the node under consideration is eliminated. E_{local} of the network provides information about network resilience to fault tolerance and is given by the average E_{global} within a local subgraph consisting only of the neighbors of a given node.

Network strength

Network strength (D) measures indicate the strength of connectivity in the corresponding network. D was calculated as the average degree over all the nodes in the network.

Assortativity

Assortativity (A) is a measure that assesses the tendency of a node being connected or disconnected to nodes of a similar degree (similar number of edges) in a network. A positive value of A indicates that nodes are likely to be connected to other nodes with the same degree and therefore hubs of the network are likely to be connected. If A is negative, this implies that the hubs of the network are not connected. A was calculated as the correlation between the degree of a node and the mean degree of its nearest neighbors.[44]

Hub disruption index

Human functional brain networks comprise several highly connected hub nodes,[34] and to investigate the potential reorganization of these hubs in the PD-FOG participants, we calculated the hub disruption index across three different groups. The hub disruption index (κ) provides a measure of change in the overall organization of brain hubs[42] and was calculated as the slope of the line fitted to the scatterplot of the average nodal strength between the reference group and the difference between the reference group and chosen group. In the current study, κ was calculated for three different comparisons: (a) the NCs as the reference group and PD-FOG as the chosen group, (b) NCs as the reference group and PD-nFOG as the chosen group, and (c) PD-nFOG as the reference group and PD-FOG as the chosen group. We used permutation testing to confirm the statistical significance ($p <$ .001) of the observed slope, that is, κ. Subjects were arbitrarily assigned to different groups and one group was defined as the reference group and the other as the chosen group and the κ was calculated using the process described above. The permutation was repeated 10,000 times to generate the null distribution of κ.

Rich-club properties

Rich-club is formed when the high-degree (nodes that have a large number of edges) nodes of a network tend to be more densely inter-connected rather than with nodes that have a lower degree. The rich-club coefficient (ϕ) was calculated as the fraction of the number of existing edges for nodes with a degree larger than k, divided by the number of possible connections among these nodes. The ϕ was normalized using 100 matched random networks (ϕ_{rand}) and the ϕ_{norm} (ϕ/ϕ_{rand}) was obtained for each participant. A value of $\phi_{norm} > 1$ over a range of k was said to reflect the existence of a rich-club organization in a network. To understand whether there is a difference in the rich-club functional organization, average rich-club edge strength, feeder edge strength, and local edge strength were then computed.[33] For each group, the presence of rich-club was assessed using the group average connectivity matrix. At the range of k where $\phi_{norm} > 1$ (ie, expressing rich-club organization), it was tested whether ϕ was significantly greater than the ϕ_{rand}. The maximum degree (k_{max}) at which $\phi > \phi_{rand}$ in all the three groups was defined as the threshold where the "rich-club" properties were obtained. At the individual subject level, all rich-club measures were

extracted and compared for differences in the rich-club properties for nodes with degrees greater than k_{max}.

Network-level differences in overall topological characteristics were studied by comparing the integrated area under the curve metrics over the whole range of S (.1:.01:.5).[39] Rich-club properties and related measures were compared at the minimum sparsity level at which the network was fully connected for all groups.[40]

The Chi-square test and the Mann-Whitney U test were used to test the significance of demographic variables, clinical variables, and head motion. All comparisons were done between the three different groups (NC vs. PD-nFOG; NC vs. PD-FOG and PD-nFOG vs. PD-FOG). Nonparametric statistical analyses of group differences in graph-based metrics and correlation with clinical variables (disease duration, FOGQ, and LEDD) were conducted using the permutation analysis of linear models (PALM) toolbox in FSL.[45] The MDS-UPDRS III score for the PD participants was included as a covariate of no interest in all of the above. Significance for PALM was established at family-wise error correction $p_{corr} < .05$.

The raw data used in the study can be downloaded from https://nevadacntn.org/. The scripts used in the study are freely available from the authors of the respective toolboxes.

RESULTS

Demographics and clinical measures

None of the demographic variables were significantly different between the groups (Table 1). All subjects had less than one voxel-size RMS head motion and this measure was not significantly different between the groups. As expected, the PD-FOG participants had significantly higher FOGQ, MDS-UPDRS-III scores, and PIGD subscores compared to the PD-nFOG participants. The LEDD was also significantly higher in PD-FOG participants. There were no between-group differences in MoCA, GDS, STAI, tremor subscore, disease duration, or Hoehn and Yahr stages (Table 1).

Altered global information processing in PD-FOG

All three groups exhibited small-world properties. However, the PD-FOG participants showed significantly reduced assortativity (A) when compared to the PD-nFOG group (Figure 1). None of the other global measures showed statistically significant differences. However, there was a trend of altered global measures in the PD-FOG group when compared to the NCs and PD-nFOG group (Figure 2).

Reorganization of functional hubs in PD-FOG

When compared to the NCs, both PD-FOG and PD-nFOG participants exhibited a significant reorganization of functional hubs as evaluated through the hub disruption index (Figure 3). The group average hub disruption index showed a significant negative slope for the NC versus PD-FOG (Figure 3A) and PD-nFOG versus PD-FOG comparisons (Figure 3C). Specifically, when comparing the PD-FOG participants against the NC, hub alterations were most evident for several regions of the visual, auditory, and sensory/motor cortex,

which all decreased their hubness. On the other hand, regions in the frontal cortex and inferior parietal lobe increased their hubness (Figure 3A). Comparison of PD-FOG and PD-nFOG revealed a similar hub reorganization. Many regions of the sensory/motor cortex and parietal cortex showed a decrease in their hubness, and regions in the frontal cortex and inferior parietal lobe displayed increased hubness (Figure 3C). The comparison between PD-nFOG and the NCs did not show significant differences (Figure 3B).

Disrupted rich-club functional organization in PD-FOG

As the network was fully connected for all three groups at a sparsity of 15%, rich-club measures were extracted and compared between groups only at this *S*. All three groups exhibited a presence of the rich-club organization. Statistically significantly ($p_{corr} < .05$) weaker feeder edge strength (Figure 4A) was found in PD-FOG when compared to PD-nFOG participants. The PD-FOG participants had a significantly higher local edge strength compared to the PD-nFOG (Figure 4B). No other differences were observed between the groups.

Correlations between clinical measures and functional network measures

There were no statistically significant findings when assessing the relationship between functional network measures and disease duration, FOGQ score, or LEDD. However, our findings did exhibit a weak relationship and differential trends in the two PD groups (Figure 5). Mainly, there was a positive relationship between assortativity and disease duration in the PD-nFOG group, whereas an inverse relationship was observed in the PD-FOG group (Figure 5a).

DISCUSSION

Utilizing well-characterized PD-FOG patients with a high-temporal-resolution rs-fMRI data on a clinical scanner, this study revealed (1) assortativity is significantly reduced in the PD-FOG group indicating altered connectivity between similar nodes (eg, hubs), (2) altered feeder network and local network measures in the PD-FOG group, (3) significant reorganization of the functional hubs in the PD-FOG group when compared to PD-nFOG and NCs, and (4) no correlations between topological measures and clinical features of PD-FOG.

This study showed that the PD-FOG participants showed significantly reduced assortativity compared to the PD-nFOG group. Assortativity is a parameter that represents the correlation of nodal degrees on either end of an edge and is considered an indirect measure of the resilience of a network.[44] In a highly assortative network, similar nodes tend to be connected and tend to be more resilient wherein the alteration of one node can be compensated by other stronger nodes. The reduced assortativity in the PD-FOG group could be an indication of aberrant connectivity between dissimilar nodes, that is, higher degree regions connected to lower degree regions. Furthermore, the PD-FOG group also showed a weak relationship between decreasing assortativity and increasing PD duration. Both these findings suggest that the topological organization of the PD-FOG group is severely affected, which may

result in inefficient between-network communication, and that this communication continues to deteriorate with PD duration.

The trends of the altered global metrics are also a supplement to the above findings. The increased clustering coefficient and reduction in path length could make the networks more “regular networks” rather than a “small-world networks” with reduced network strength. Subsequently, the networks are unable to efficiently transfer the information as might be observed from the trends of reduced global and local efficiency.

In line with the observed alternations in the assortativity in the PD-FOG participants, there was also a marked reorganization of “hub” regions as revealed by the hub disruption index. This nodal reorganization was not significantly different when comparing NCs and PD-nFOG participants. The comparison between NCs and the PD-FOG participants showed that parietal and occipital regions with high nodal connectivity (hub regions) exhibited greatly reduced functional interactions (non-hub-like), while the frontal regions demonstrated a notable increase (hub-like) in their functional interactions in the FOG participants. However, more importantly, compared to the PD-nFOG group, regions that are part of the primary somatosensory, motor (eg, postcentral gyrus, paracentral lobule), and visuomotor coordination areas (eg, superior parietal lobule) showed a substantial reduction in hubness in the PD-FOG participants. Furthermore, regions belonging to the prefrontal cortex namely the superior frontal, middle frontal, and inferior frontal regions showed an increase in their hubness in PD-FOG compared to PD-nFOG participants.

The impairment of the FPN observed in our study is in line with previous neuroimaging studies that have consistently identified structural and functional changes in the FPN in PD-FOG.[13] FPN dysfunction has been consistently associated with FOG in PD and is currently hypothesized as a key mechanism pertinent to the development of PD-FOG.[13] Significant alterations in bold response and FC among the regions that are a part of the FPN have been reported in PD-FOG.[13,46] Evidence from several clinical and neuropsychological studies also shows that PD-FOG correlates with aberrations in executive functions such as response inhibition, problem-solving, and divided or switching attention.[9,13] Divided or switching attention plays a relevant role in locomotion[47] and subsequently, executive and attention deficits could contribute to deficits in set-shifting and therefore to FOG during tasks involving high cognitive demand. The results of our study also indicate a significant increase in hubness in the regions that are part of the prefrontal cortex and can be attributed to increased demand in cortical functioning due to deficits in movement automaticity in PD-FOG.[48]

Given previous evidence that FPN may serve as a flexible hub that alters FC with other neural networks based on task requirements,[49] as well as its proposed role in cognitive and executive functioning that is associated with PD-FOG,[50] the observed changes in hub-like characteristics of several frontal and parietal regions in the PD-FOG group in our study indicate the importance of these regions in the communication between the different neural networks in situations of increased cognitive demands during gait. Hub regions not only play an important role in localized information processing (segregation) but are involved in the integration of information across the cortical brain network.[34] The organizational properties

of the hubs can be studied by the “rich-club” phenomenon where hubs of a network tend to be more connected to similar nodes (hubs) rather than nodes of a lower degree (non-hubs).[33]

The rich-club organization can provide important information related to the higher order topological organization of the brain’s functional networks. To this end, we observed that all three groups (PD-FOG, PD-nFOG, and NC) showed the existence of the rich-club organization. However, there was a significant decrease in the feeder edge strength in the PD-FOG group when compared to the PD-nFOG group. The local connectivity (the connection between non-hubs) was significantly higher in the PD-FOG group when compared to PD-nFOG. In parallel with the reduced assortativity and reorganization of hubs, the alterations in the feeder and local connectivity indicate a disturbance in between-network integration required for higher level functions. These results suggest the failure in effective integration of information between these hub regions leading to deficits in dual-tasking ability or inability to “set-shift” among the different neural networks. Existing evidence on the alterations of the brain’s functional rich-club organization in neurodegenerative disorders[51–53] further supports the importance of studying the higher level architectural organization of the brain in PD-FOG.

Limitations of this study should be noted. First, FOG in PD is a complex issue on multiple levels, and recognizing that it is not a uniform and homogeneous symptom is crucial to gaining a better understanding of its pathophysiology.[2] FOG can be classified based on response to medication as follows: (a) levodopa responsive (FOG only in the “OFF” state), (b) levodopa unresponsive, and (c) levodopa induced (FOG only in the “ON” state).[2,54–55] In this study, we did not classify PD patients based on their response to medication. Also, we investigated the differences in the clinically defined “ON’ state and as a result, our findings may not provide a comprehensive analysis of the functional disturbances that exist before dopamine supplementation in the “OFF” state. Hence, to be able to fully understand the underlying pathophysiology and the different pharmacological FOG subtypes, future studies should (a) compare the different subtypes and (b) investigate levodopa-dependent brain connectivity. Second, our PD-FOG group had a higher MDS-UPDRS-III score when compared to the PD-nFOG group. However, we believe that our results are not primarily driven by this since (a) the two groups were not significantly different in age, PD duration, tremor subscore, or Hoehn and Yahr stage, and (b) earlier studies have shown that higher disability (measured by MDS-UPDRS-III scores) is a clinical feature of FOG[2] and (c) the MDS-UPDRS-III scores were used as a covariate of no interest in all the comparisons. However, these findings point to measures and outcomes to be further explored with more closely matched samples to further understand the biology of FOG. Third, there is a possibility that changes in the “hubness” of frontal and parietal regions seen in PD-FOG participants could be associated with cognitive decline. In addition, FOG pharmacological subtypes can also exhibit different cognitive profiles.[56] While our PD-FOG and PD-nFOG participants showed no differences in the MoCA, GDS, or STAI scores, our study did not conduct a detailed evaluation of the relationship between network changes and cognition. Fourth, our study also does not conclusively provide evidence to support or oppose any of the four common hypotheses. Future studies should understand the changes in the topological organization when the participants are doing an FOG-inducing task in the scanner.[10,12] Finally, we did not observe any statistically significant relationship between

the network measures and clinical measures. However, a weak correlation and difference in the relationships were observed between some of the global network measures and clinical measures (Figure 5). Therefore, further follow-up studies of larger sample sizes with deeper phenotyping are required to confirm our findings. Such studies may allow the detection of significant differences and relationships between connectivity and behavior (including detailed cognitive assessments) that were not observed in the current data set.

Future directions to be explored to gain further understanding of the pathophysiology of FOG include (a) studying the strength of network division using modularity measures to shed more insights into the inability to shift between networks, (b) elucidating FOG subtypes based on rs-FC and network topology, (c) studying the effect of levodopa by comparing “ON” and “OFF” state network topology in PD-FOG, (d) examining the FC during the performance of specific executive-attention tasks, (e) incorporating advanced analytical methods like dynamic FC[57] and empirical mode decomposition,[58,59] and (f) conducting joint analysis of structural network connectivity disturbance[60] and functional network connectivity disturbance.

In summary, the results of our study demonstrate that PD-FOG participants exhibit different pathophysiology compared to PD-nFOG and NC due to the substantial reorganization of regional brain hubs. In addition, there was a significant reduction in the rich-club connectivity strength in the PD-FOG participants suggestive of disruptions in the higher order functional network topology.

ACKNOWLEDGMENTS

We would like to acknowledge Dr. David Standaert and Dr. Natividad Stover from The University of Alabama at Birmingham for critically reviewing our manuscript.

Funding information

NIH, Grant/Award Numbers: R01NS117547, 1RF1AG071566, 1P20GM109025-01A1; Elaine P Wynn and Family Foundation; Peter and Angela Dal Pezzo; Lynn and William Weidner; Stacie and Chuck Matthewson and the Keep Memory Alive-Young Investigator Award

REFERENCES

1. Allen NE, Schwarzel AK, Canning CG. Recurrent falls in Parkinson’s disease: a systematic review. Parkinsons Dis. 2013;2013:906274. [PubMed: 23533953]
2. Amboni M, Stocchi F, Abbruzzese G, et al. Prevalence and associated features of self-reported freezing of gait in Parkinson disease: the DEEP FOG study. Parkinsonism Relat Disord. 2015;21:644–9. [PubMed: 25899545]
3. Macht M, Kaussner Y, Möller JC, et al. Predictors of freezing in Parkinson’s disease: a survey of 6,620 patients. Mov Disord. 2007;22:953–6. [PubMed: 17377927]
4. Snijders AH, Leunissen I, Bakker M, et al. Gait-related cerebral alterations in patients with Parkinson’s disease with freezing of gait. Brain. 2011;134:59–72. [PubMed: 21126990]
5. Plotnik M, Giladi N, Hausdorff JM. Is freezing of gait in Parkinson’s disease a result of multiple gait impairments? Implications for treatment. Parkinsons Dis. 2012;2012:459321. [PubMed: 22288021]
6. Lewis SJG, Barker RA. A pathophysiological model of freezing of gait in Parkinson’s disease. Parkinsonism Relat Disord. 2009;15:333–8. [PubMed: 18930430]
7. Vandenbossche J, Deroost N, Soetens E, et al. Freezing of gait in Parkinson’s disease: disturbances in automaticity and control. Front Hum Neurosci. 2012;6:356. [PubMed: 23335895]

8. Jacobs JV, Nutt JG, Carlson-Kuhta P, et al. Knee trembling during freezing of gait represents multiple anticipatory postural adjustments. Exp Neurol. 2009;215:334–41. [PubMed: 19061889]
9. Bluett B, Banks S, Cordes D, et al. Neuroimaging and neuropsychological assessment of freezing of gait in Parkinson's disease. Alzheimers Dement. 2018;4:387–94.
10. Shine JM, Matar E, Ward PB, et al. Freezing of gait in Parkinson's disease is associated with functional decoupling between the cognitive control network and the basal ganglia. Brain. 2013;136:3671–81. [PubMed: 24142148]
11. Browner N, Giladi N. What can we learn from freezing of gait in Parkinson's disease? Curr Neurol Neurosci Rep. 2010;10: 345–51. [PubMed: 20559757]
12. Naismith SL, Shine JM, Lewis SJG. The specific contributions of set-shifting to freezing of gait in Parkinson's disease. Mov Disord. 2010;25:1000–4. [PubMed: 20198644]
13. Bharti K, Suppa A, Tommasin S, et al. Neuroimaging advances in Parkinson's disease with freezing of gait: a systematic review. Neuroimage Clin. 2019;24:102059. [PubMed: 31795038]
14. Fasano A, Herman T, Tessitore A, et al. Neuroimaging of freezing of gait. J Parkinsons Dis. 2015;5:241–54. [PubMed: 25757831]
15. Ruan X, Li Y, Li E, et al. Impaired topographical organization of functional brain networks in Parkinson's disease patients with freezing of gait. Front Aging Neurosci. 2020;12:337.
16. Maidan I, Jacob Y, Giladi N, et al. Altered organization of the dorsal attention network is associated with freezing of gait in Parkinson's disease. Parkinsonism Relat Disord. 2019;63:77–82. [PubMed: 30827838]
17. Bullmore E, Sporns O. Complex brain networks: graph theoretical analysis of structural and functional systems. Nat Rev Neurosci. 2009;10:186–98. [PubMed: 19190637]
18. Sporns O, Tononi G, Kötter R. The human connectome: a structural description of the human brain. PLoS Comput Biol. 2005;1:e42. [PubMed: 16201007]
19. Bassett DS, Bullmore E, Verchinski BA, et al. Hierarchical organization of human cortical networks in health and Schizophrenia. J Neurosci. 2008;28:9239–48. [PubMed: 18784304]
20. Achard S, Salvador R, Whitcher B, et al. A resilient, low-frequency, small-world human brain functional network with highly connected association cortical hubs. J Neurosci. 2006;26:63–72. [PubMed: 16399673]
21. Cao M, Huang H, He Y. Developmental connectomics from infancy through early childhood. Trends Neurosci. 2017;40:494–506. [PubMed: 28684174]
22. Perry A, Wen W, Lord A, et al. The organisation of the elderly connectome. Neuroimage. 2015;114:414–26. [PubMed: 25869857]
23. Bachmann C, Jacobs HIL, Porta Mana P, et al. On the extraction and analysis of graphs from resting-state fMRI to support a correct and robust diagnostic tool for Alzheimer's disease. Front Neurosci. 2018;12:528. [PubMed: 30323734]
24. Rocca MA, Valsasina P, Meani A, et al. Impaired functional integration in multiple sclerosis: a graph theory study. Brain Struct Funct. 2016;221:115–31. [PubMed: 25257603]
25. Gleichgerrcht E, Kocher M, Bonilha L. Connectomics and graph theory analyses: novel insights into network abnormalities in epilepsy. Epilepsia. 2015;56:1660–8. [PubMed: 26391203]
26. Caliandro P, Vecchio F, Miraglia F, et al. Small-world characteristics of cortical connectivity changes in acute stroke. Neurorehabil Neural Repair. 2017;31:81–94. [PubMed: 27511048]
27. Caeyenberghs K, Verhelst H, Clemente A, et al. Mapping the functional connectome in traumatic brain injury: what can graph metrics tell us? Neuroimage. 2017;160:113–23. [PubMed: 27919750]
28. Mishra VR, Sreenivasan KR, Yang Z, et al. Unique white matter structural connectivity in early-stage drug-naive Parkinson disease. Neurology. 2020;94:e774–84. [PubMed: 31882528]
29. Sreenivasan K, Mishra V, Bird C, et al. Altered functional network topology correlates with clinical measures in very early-stage, drug-naïve Parkinson's disease. Parkinsonism Relat Disord. 2019;62:3–9. [PubMed: 30772280]
30. Rubinov M, Sporns O. Complex network measures of brain connectivity: uses and interpretations. Neuroimage. 2010;52:1059–69. [PubMed: 19819337]
31. Li N, Suo X, Zhang J, et al. Disrupted functional brain network topology in Parkinson's disease patients with freezing of gait. Neurosci Lett. 2021;759:135970. [PubMed: 34023405]

32. Guo MR, Ren Y, Yu HM, et al. Alterations in degree centrality and functional connectivity in Parkinson's disease patients with freezing of gait: a resting-state functional magnetic resonance imaging study. Front Neurosci. 2020;14:582079. [PubMed: 33224024]
33. van den Heuvel MP, Sporns O. Rich-club organization of the human connectome. J Neurosci. 2011;31:15775–86. [PubMed: 22049421]
34. van den Heuvel MP, Sporns O. Network hubs in the human brain. Trends Cogn Sci. 2013;17:683–96. [PubMed: 24231140]
35. Gibb WR, Lees AJ. The relevance of the Lewy body to the pathogenesis of idiopathic Parkinson's disease. J Neurol Neurosurg Psychiatry. 1988;51:745–52. [PubMed: 2841426]
36. Ziegler K, Schroeteler F, Ceballos-Baumann AO, et al. A new rating instrument to assess festination and freezing gait in Parkinsonian patients. Mov Disord. 2010;25:1012–8. [PubMed: 20310009]
37. Fan L, Li H, Zhuo J, et al. The Human Brainnetome Atlas: a new brain atlas based on connectional architecture. Cereb Cortex. 2016;26:3508–26. [PubMed: 27230218]
38. Behzadi Y, Restom K, Liau J, et al. A component based noise correction method (CompCor) for BOLD and perfusion based fMRI. Neuroimage. 2007;37:90–101. [PubMed: 17560126]
39. Achard S, Bullmore E. Efficiency and cost of economical brain functional networks. PLoS Comput Biol. 2007;3: e17. [PubMed: 17274684]
40. He Y, Chen Z, Evans A. Structural insights into aberrant topological patterns of large-scale cortical networks in Alzheimer's disease. J Neurosci. 2008;28:4756–66. [PubMed: 18448652]
41. Wang J, Wang X, Xia M, et al. GRETNA: a graph theoretical network analysis toolbox for imaging connectomics. Front Hum Neurosci. 2015;9:386. [PubMed: 26175682]
42. Achard S, Delon-Martin C, Vértes PE, et al. Hubs of brain functional networks are radically reorganized in comatose patients. Proc Natl Acad Sci USA. 2012;109:20608–13. [PubMed: 23185007]
43. Watts DJ, Strogatz SH. Collective dynamics of 'small-world' networks. Nature. 1998;393:440–2. [PubMed: 9623998]
44. Newman MEJ. Assortative mixing in networks. Phys Rev Lett. 2002;89:208701. [PubMed: 12443515]
45. Winkler AM, Ridgway GR, Webster MA, et al. Permutation inference for the general linear model. Neuroimage. 2014;92:381–97. [PubMed: 24530839]
46. Shine JM, Moustafa AA, Matar E, et al. The role of frontostriatal impairment in freezing of gait in Parkinson's disease. Front Syst Neurosci. 2013;7:61. [PubMed: 24109438]
47. Mirelman A, Shema S, Maidan I, et al. Gait. Handb Clin Neurol. 2018;159:119–34. [PubMed: 30482309]
48. Nieuwboer A, Giladi N. Characterizing freezing of gait in Parkinson's disease: models of an episodic phenomenon. Mov Disord. 2013;28:1509–19. [PubMed: 24132839]
49. Cole MW, Reynolds JR, Power JD, et al. Multi-task connectivity reveals flexible hubs for adaptive task control. Nat Neurosci. 2013;16:1348–55. [PubMed: 23892552]
50. Zanto TP, Gazzaley A. Fronto-parietal network: flexible hub of cognitive control. Trends Cogn Sci. 2013;17:602–3. [PubMed: 24129332]
51. He Y, Chen Z, Gong G, et al. Neuronal networks in Alzheimer's disease. Neuroscientist. 2009;15:333–50. [PubMed: 19458383]
52. Kambeitz J, Kambeitz-Ilankovic L, Cabral C, et al. Aberrant functional whole-brain network architecture in patients with schizophrenia: a meta-analysis. Schizophr Bull. 2016;42:S13–21. [PubMed: 27460615]
53. Dicks E, Tijms BM, ten Kate M, et al. Gray matter network measures are associated with cognitive decline in mild cognitive impairment. Neurobiol Aging. 2018;61:198–206. [PubMed: 29111486]
54. Espay AJ, Fasano A, Van Nuenen BFL, et al. "On" state freezing of gait in Parkinson disease: a paradoxical levodopa-induced complication. Neurology. 2012;78:454–7. [PubMed: 22262741]
55. Fasano A, Lang AE. Unfreezing of gait in patients with Parkinson's disease. Lancet Neurol. 2015;14:675–7. [PubMed: 26018594]

56. Factor SA, Scullin MK, Sollinger AB, et al. Freezing of gait subtypes have different cognitive correlates in Parkinson's disease. Parkinsonism Relat Disord. 2014;20:1359–64. [PubMed: 25446341]

57. Zhuang X, Walsh RR, Sreenivasan K, et al. Incorporating spatial constraint in co-activation pattern analysis to explore the dynamics of resting-state networks: an application to Parkinson's disease. Neuroimage. 2018;172:64–84. [PubMed: 29355770]

58. Cordes D, Zhuang X, Kaleem M, et al. Advances in functional magnetic resonance imaging data analysis methods using empirical mode decomposition to investigate temporal changes in early Parkinson's disease. Alzheimers Dement. 2018;4:372–86.

59. Cordes D, Kaleem MF, Yang Z, et al. Energy-period profiles of brain networks in group fMRI resting-state data: a comparison of empirical mode decomposition with the short-time Fourier transform and the discrete wavelet transform. Front Neurosci. 2021;15:594.

60. Mishra V, Sreenivasan K, Bird C, et al. Distinct structural backbone-network in early Parkinson's disease (PD) subjects: insights from Parkinson's Progressive Markers Initiative (PPMI) dataset. Presented at the 25th Annual Meeting for the International Society for Magnetic Resonance in Medicine; April 27, 2017; Honolulu.

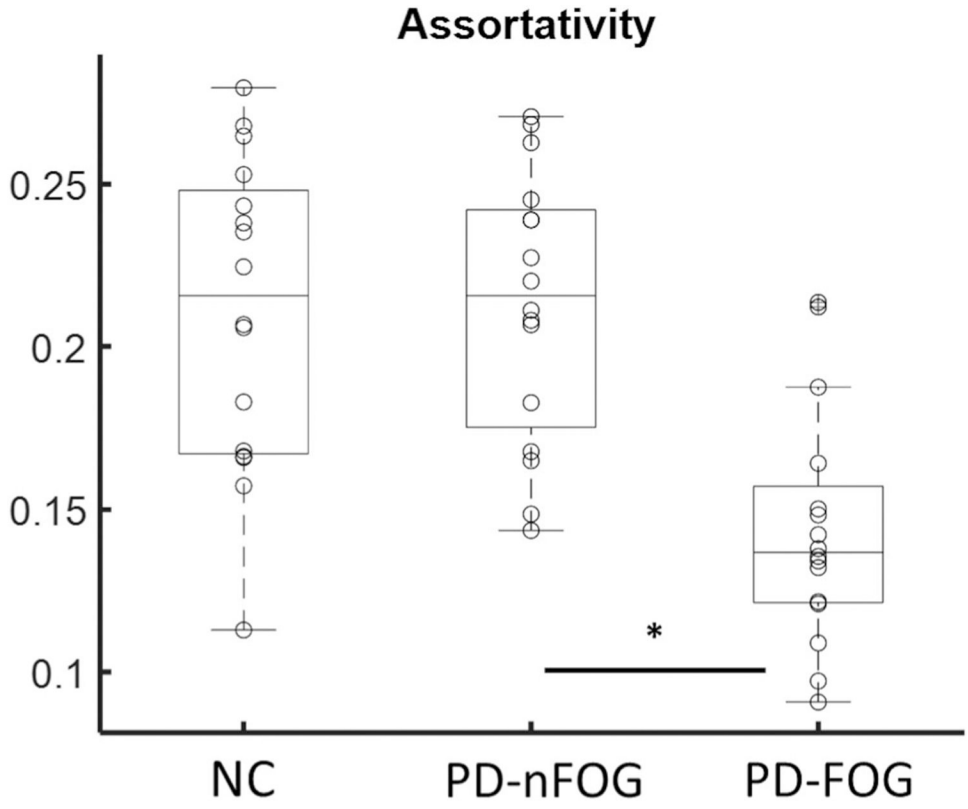

FIGURE 1.

Significantly altered global assortativity in the PD-FOG group. An asterisk (*) indicates significant (corrected $p < .05$) difference. The *y*-axis in the figure is the assortativity measure. NC, normal controls; PD-nFOG, Parkinson's disease patients without freezing of gait; PD-FOG, Parkinson's disease patients with freezing of gait. The red data points in the plot represent potential outliers.

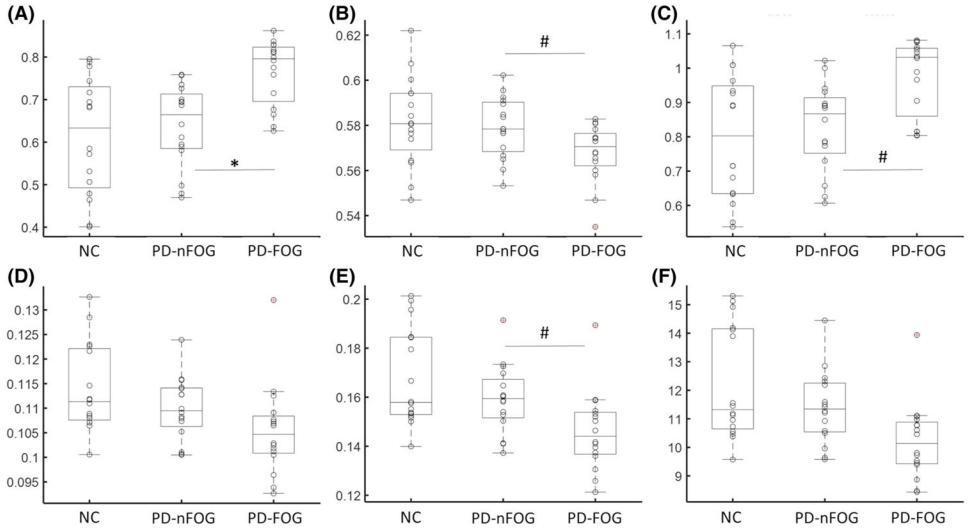

FIGURE 2.

Global network metrics in the study groups. (A) Small-worldness, (B) path length, (C) clustering coefficient, (D) global efficiency, (E) local efficiency, and (F) strength. The *y*-axis denotes the values of the global network metric as represented in the title of the subplot. The hash symbol (#) indicates uncorrected $p < .05$. NC, normal controls; PD-nFOG, Parkinson's disease patients without freezing of gait; PD-FOG, Parkinson's disease patients with freezing of gait. The red data points in the plot represent potential outliers.

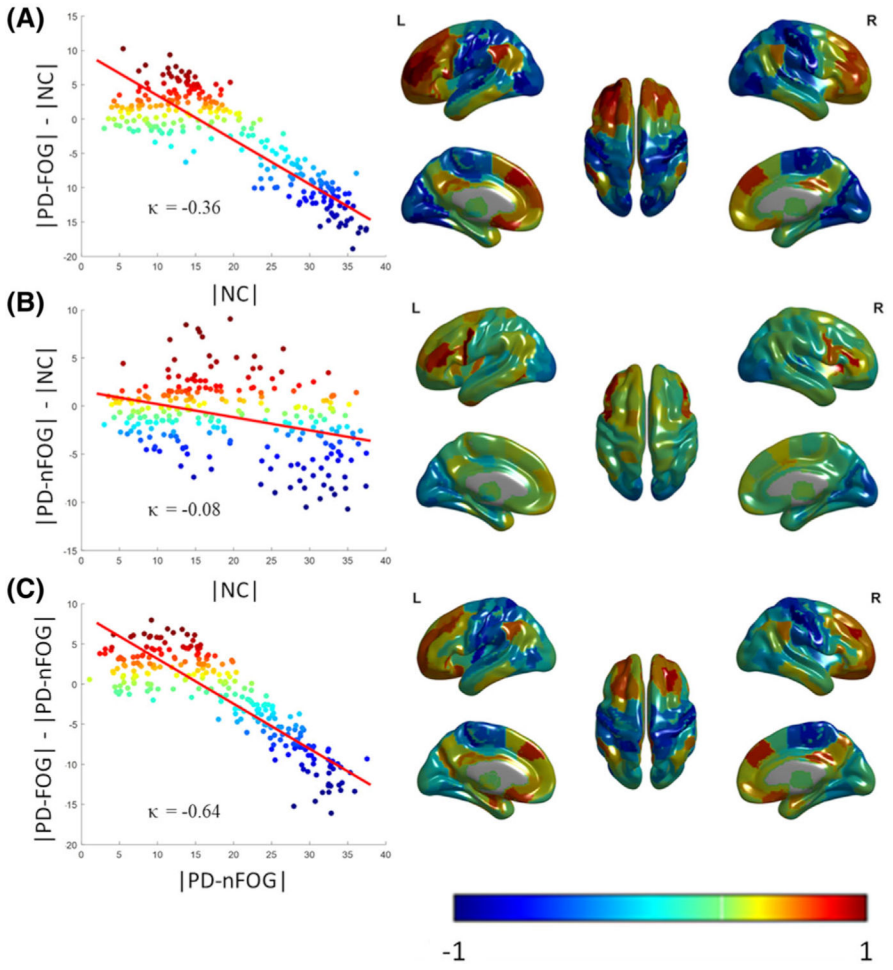

FIGURE 3.

The hub regions were significantly reorganized in the PD-FOG participants. The mean degree of each node in the reference group (*x*-axis) is plotted versus the difference between the mean degree of each node of the reference group and chosen group (*y*-axis). Hub disruption index (κ) was calculated as the slope of the line (shown in red) fitted to the scatterplot. (A) Reference group: control (NC); chosen group: PD-FOG. (B) Reference group: NC; chosen group: PD-nFOG. (C) Reference group: PD-nFOG; chosen group: PD-FOG. The red color denotes increased hubness, on average, in the chosen group compared to the reference group; blue denotes abnormally decreased hubness in the chosen group. The right panel in each of the subfigures is the cortical surface representation of the difference in mean degree between the reference and chosen group and the colors are the same as in the scatter plot. L, left; R, right.

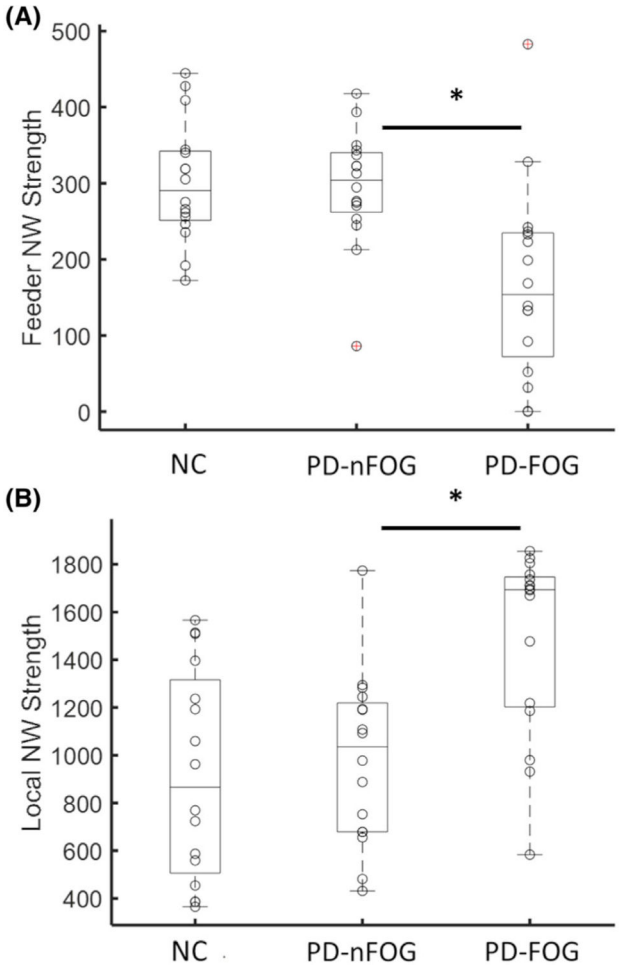

FIGURE 4.

Rich-club connectivity in the three study groups. (A) Feeder network strength and (B) local network strength are plotted as bar plots for the different groups. An asterisk (*) indicates statistical significance (corrected $p < .05$). NC, normal controls; PD-nFOG, Parkinson's disease patients without freezing of gait; PD-FOG, Parkinson's disease patients with freezing of gait; NW, network. Feeder network—edges connecting non-rich-club nodes and rich-club nodes; local network—edges between non-rich-club nodes. The red data points in the plot represent potential outliers.

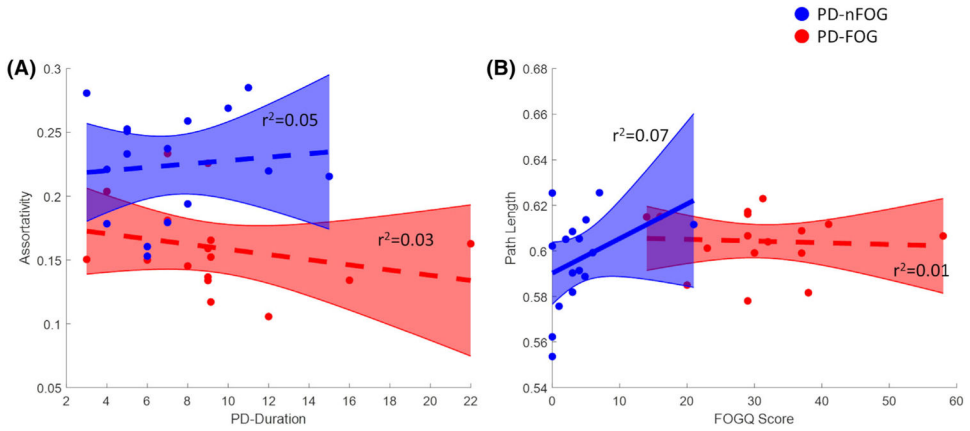

FIGURE 5.

Relationship between network measures and clinical measures. The correlation between (A) assortativity and PD duration (in years), and (B) path length and Freezing of Gait Questionnaire (FOGQ). The solid line indicates uncorrected $p < .05$ and the dashed line indicates $p > .05$. PD-nFOG, Parkinson's disease patients without freezing of gait; PD-FOG, Parkinson's disease patients with freezing of gait.

TABLE 1

Demographics.

Demographics	Controls (*n* = 16)	PD-nFOG (*n* = 16)	PD-FOG (*n* = 16)	*p*-value
Age (Years)	68.50 ± 4.29	67.56 ± 6.63	69.43 ± 7.22	.73
Sex(M: Males; F: Females)	9 M; 7 F	10 M; 6 F	13 M; 3 F	.29
Handedness R = Right-handed; L = Left-handed	16 R	14 R; 2 L	15 R; 1 L	.34
Years of education	16.19 ± 1.47	16.19 ± 2.19	14.93 ± 2.41	.14
Montreal Cognitive Assessment	26.50 ± 2.66	26.37 ± 2.47	24.75 ± 2.41	.07
Geriatric Depression Scale	-	5.69 ± 6.80	9.56 ± 7.07	.06
State-Trait Anxiety Inventory (State Anxiety)	-	32.05 ± 10.67	32.81 ± 10.02	.47
State-Trait Anxiety Inventory (Trait Anxiety)	-	31.24 ± 9.85	36.5 ± 10.89	.08
Hoehn and Yahr scale (1/2/3)	-	0/16/0	0/13/3	.07
Disease duration	-	7.25 ± 3.29	9.48 ± 4.56	.10
Levodopa equivalent doses	-	490.54 ± 258.56	1052.03 ± 597.08	.001*
Freezing of Gait Questionnaire	-	2.36 ± 3.11	14.35 ± 3.09	<.001*
MDS-Unified Parkinson's Disease RatingScale-III (ON-state)	-	18.12 ± 3.65	25.53 ± 7.72	.001*
Postural instability/gait disturbance (gait, freezing of gait, postural stability)	-	0.69 ± 0.48	2.27 ± 2.12	.01*
Tremor score (postural tremor RUE/LUE, kinetic tremor RUE/LUE, rest tremor RUE/LUE/RLE/LLE, rest tremor lip/jaw, rest constancy)	-	3.63 ± 2.39	2.87 ± 2.59	.22

Note: Various demographics, clinical scores, and Movement Disorders Society (MDS)-Unified Parkinson's Disease Rating Scale-III in ON state (Parkinson's disease subjects only) are shown along with their mean ± standard deviation. Statistical comparison was conducted between the groups for all clinical and demographical variables using either the Chi-square test (for values in categorical scale) or the Mann-Whitney test (for values in continuous scale) and are shown as *p*-values. An asterisk indicates a significant difference $p < .05$. *n* represents the sample size.

Abbreviations: LLE, left lower extremity; LUE, left upper extremity; *n*, sample size; RLE, right lower extremity; RUE, right upper extremity.